Hindawi Publishing Corporation
Journal of Nanomaterials
Volume 2014, Article ID 876571, 6 pages
http://dx.doi.org/10.1155/2014/876571

Research Article

Anodic CaO-TiO_2 Nanotubes Composite Film for Low Temperature CO_2 Adsorption

Chin Wei Lai

Nanotechnology & Catalysis Research Centre (NANOCAT), Institute of Postgraduate Studies (IPS), Universiti Malaya, 3rd Floor, Block A, 50603 Kuala Lumpur, Malaysia

Correspondence should be addressed to Chin Wei Lai; cwlai@um.edu.my

Received 12 January 2014; Revised 8 April 2014; Accepted 9 April 2014; Published 4 May 2014

Academic Editor: Sun-Hwa Yeon

A novel one-dimensional anodic CaO-TiO_2 nanotubes composite film was prepared using a rapid-anodic oxidation electrochemical anodization technique for low temperature CO_2 absorption application. This study aims to determine the optimum concentration of $Ca(NO_3)_2{\cdot}4H_2O$ used as the CaO precursor for loading CaO species on TiO_2 nanotubes. In this study, an optimum content of CaO on TiO_2 nanotubes (0.15 at% of Ca element) could enhance the CO_2 adsorption capacity up to 2.45 mmol/g at 400°C. This behavior was attributed to the large active surface area of CaO species were covered on the surface of TiO_2 nanotubes. The conversion of CaO into $CaCO_3$ could be achieved effectively for CO_2 absorption during the carbonate looping process.

1. Introduction

Nowadays, carbon dioxide (CO_2) has become the focus of attention as the primary greenhouse gas in the atmosphere which leads to the global warming [1]. The increasing of CO_2 emission in atmosphere is leading to global warming and climate change [1, 2]. The fossil fuels supply more than 98% of the world's energy needs and the combustion of the fossils fuels is one of the major sources of the greenhouse gas [3]. It is necessary to reduce the emission of this gas. Several options are available to reduce these CO_2 emissions, including substitution of nuclear power and natural gas for fossil fuels and coal, separating and capturing CO_2 prior to emission into atmosphere [4]. Nowadays, the CO_2 emission is almost 390 parts per million (ppm) which is above the safety limit of 350 ppm [2, 5]. Therefore, developments of carbon capturing work have become very significant option to stop and reduce the CO_2 emission. Malaysia as one of the ASEAN countries had agreed to reduce the CO_2 emission up to 40% by year of 2020. In fact, there are several advance technologies to capture CO_2, such as chemical (gas-liquid) adsorption, adsorption, cryogenic separation, membrane separation, and biological fixation [6]. Among all of these listed technologies, adsorption is a promising heterogeneous process that can separate CO_2 from the fuel gases of coal-fired power plants effectively [6, 7]. These CO_2 molecules can be captured on the surface of the sorbents effectively because of the interaction between sorbent and CO_2 gas [5]. In general, CO_2 adsorption process is very stable and has high cyclic capture capacities and low energy consumption for regeneration in comparison to aqueous systems. The adsorption kinetics depend on temperature, pressure, interaction energy between sorbent and CO_2 on the surface, and pore size or surface area of the adsorbents [2, 5, 6].

Nevertheless, the conventional CO_2 adsorbents used suffer severe degradation during their operations of sorption and desorption [8]. These conventional CO_2 adsorbents usually can only run several tens of cycles before showing obvious degradation. The deactivation primary resulted from the formation of thin $CaCO_3$ layer surrounding the CaO surface. Once a certain thickness of 20 nm $CaCO_3$ is reached, the diffusion of CO_2 will be hindered to react with CaO inner core [6, 8]. Thus, continuous efforts have been exerted to further improve the CaO texture and structure by designing its architecture in one-dimensional nanoscale for high efficiency in capturing the CO_2. Recent studies have indicated that one-dimensional nanotubular structure is able to provide a higher active surface area (inner and outer surface) for carbonate

looping process [9–11]. However, the literature regarding the formation of one-dimensional CaO nanoarchitecture was limited. Thus, innovative new approaches and synthesis of a high quality one-dimensional CaO-TiO_2 nanoarchitecture are crucial for determining the potential of the material as efficient CO_2 adsorbents. The CaO-TiO_2 nanoarchitecture composite film is believed to have its own unique characteristics, such as high selectivity and adsorption capacity for CO_2, fast adsorption and desorption kinetics, stable cyclic adsorption capacity, and low energy needs for regeneration of pure CO_2 [2].

Herein, we report the formation of CaO-TiO_2 nanoarchitecture composite film using a simple electrochemical anodization method for high CO_2 adsorption capacity. The electrochemical anodization method is a compromising synthetic technique to grow the one-dimensional nanoarchitecture because of its low cost, mild conditions, and accurate process control [12]. Thus, the controlled growth of CaO-TiO_2 nanoarchitecture composite film is our innovation to further improve CO_2 adsorption capacity and adopted for large-scale industrial production. Meanwhile, the ultimate aim of the present work is to form well-aligned CaO-TiO_2 nanotubes composite film, which is able to perform CO_2 adsorption at low temperature of 400°C.

2. Experimental Procedure

The self-organized TiO_2 nanotubes film was synthesized from a rapid-anodic oxidation electrochemical anodization of a high purity Ti foil (99.6%, Strem Chemical, USA) with a thickness of 127 μm with surface area of about 10 cm^2. This process was conducted in a bath with electrolytes composed of ethylene glycol ($C_2H_6O_2$, >99.5%, Merck, USA), 5 wt% ammonium fluoride (NH_4F, 98%, Merck, USA), and 5 wt% hydrogen peroxide (H_2O_2, 30% H_2O_2 and 70% H_2O, J.T. Baker, USA), as well as different concentrations of calcium nitrate tetrahydrate ($Ca(NO_3)_2{\cdot}4H_2O$, Merck, USA). The concentrations of $Ca(NO_3)_2{\cdot}4H_2O$ were varied from 0.01 M up to 0.10 M. This process was carried out for 60 minutes at a constant potential of 60 V using a Keithley DC power supply. When the circuit was closed, external potential bias was generated and then the current moved from the positive terminal (platinum rod) to the negative terminal (Ti foil). Before synthesis, the distance between anode and cathode was fixed at 30 mm. After the anodization process, as-anodized samples were cleaned using distilled water and dried under a nitrogen (N_2) stream. The resultant samples were then thermally annealed at 400°C in argon atmosphere for 4 h.

The morphologies of the resultant samples were characterized using field emission scanning electron microscopy (FESEM, Zeiss SUPRA 35VP, Germany) operating at 5 kV. The elemental analysis, that is, atomic percentage of samples, can be determined by energy dispersion X-ray (EDX), which is equipped in the FESEM. The crystal structure and phase present in samples were determined using X-ray diffraction (XRD). The thermogravimetric analysis (TGA) was used to investigate the CO_2 adsorption using CaO-TiO_2 composite film. The CO_2 adsorption capacity could be identified through the carbonation/regeneration process via TGA curves (STA 6000, Perkin Elmer, USA). The carbonation process can be defined as $CaO + CO_2 \rightarrow CaCO_3$ (400°C), whereas the regeneration process can be defined as $CaCO_3 \rightarrow CaO + CO_2$ (300°C). A N_2 gas flow at a rate of 10°C/min from room temperature to 400°C, and then hold for 30 min in CO_2, finally cool down to 300°C by N_2 gas. The carbonation is set to be 400°C because TiO_2 nanotubes will collapse due to the effects of high temperature (above 500°C) and phase transition heat problems [13].

3. Results and Discussion

A preliminary experiment was carried out by adopting optimized laboratory conditions to grow TiO_2 nanotubes in $C_2H_6O_2$ electrolyte containing 5 wt% of H_2O_2 and 5 wt% of NH_4F. The electrochemical anodization voltage was kept at 60 V for 60 minutes and the pH of this electrolyte was maintained at 6.5. Based on our preliminary studies, this selected composition of electrolyte was favored to form the highly ordered and well-aligned nanotubular structure [14–16]. The top and cross-sectional view of pure TiO_2 nanotubes before incorporating with $Ca(NO_3)_2{\cdot}4H_2O$ dopants are illustrated in Figure 1(a). The vertical growth of TiO_2 nanotubular structure on Ti substrate could be observed clearly. The nanotubular structure has an average diameter of 110 nm and an average length of 10 μm. Then, the experimental works were continued by implementing the optimized condition to form CaO-TiO_2 nanotubes composite film with addition of different concentrations of $Ca(NO_3)_2{\cdot}4H_2O$ to electrolyte. In this case, the calcium ions (Ca^{2+}) within the electrolyte were deposited on TiO_2 nanotubes. These Ca^{2+} ions were then converted into calcium oxide (CaO) for the formation of CaO-TiO_2 nanotubes, where dissolved Ca^{2+} ions reacted with oxygen species. The FESEM images of the synthesized CaO-TiO_2 nanotubes composite film with different concentrations of $Ca(NO_3)_2{\cdot}4H_2O$ are presented in Figures 1(b) to 1(d). All of these FESEM images showed that the appearance of the nanotubular structure was dependent on the concentration of $Ca(NO_3)_2{\cdot}4H_2O$. The morphology of CaO-TiO_2 nanotubes composite film synthesized in 0.01 M presented similar appearance to the pure TiO_2 nanotubes (Figure 1(b)). This observation manifested that the small Ca^{2+} ions might be diffused into the lattice of TiO_2 significantly. Generally, amorphous TiO_2 has several defects such as oxygen-deficient defects, point defects (cationic vacancy), impurities, and microvoids to provide a better side for deposition of Ca^{2+} ions [17, 18]. Next, the average atomic percentage (at%) of the elements in the pure TiO_2 nanotubes was determined using EDX analysis. The numerical EDX analyses of the samples are listed in Table 1. The pure TiO_2 nanotubes were mainly composed of 35.37 at% Ti, 56.48 at% O, and 8.15 at% C. Notably, the incorporation of the carbon species into the nanotubular structure was identified from the pyrogeneration of organic electrolyte (ethylene glycol, $C_3H_6O_2$) during the electrochemical anodization stage [19]. As the concentration of $Ca(NO_3)_2{\cdot}4H_2O$ was increased to 0.05 M, most of the TiO_2 pore entrances were clogged with the CaO species as indicated in Figure 1(c). Moreover, a different surface

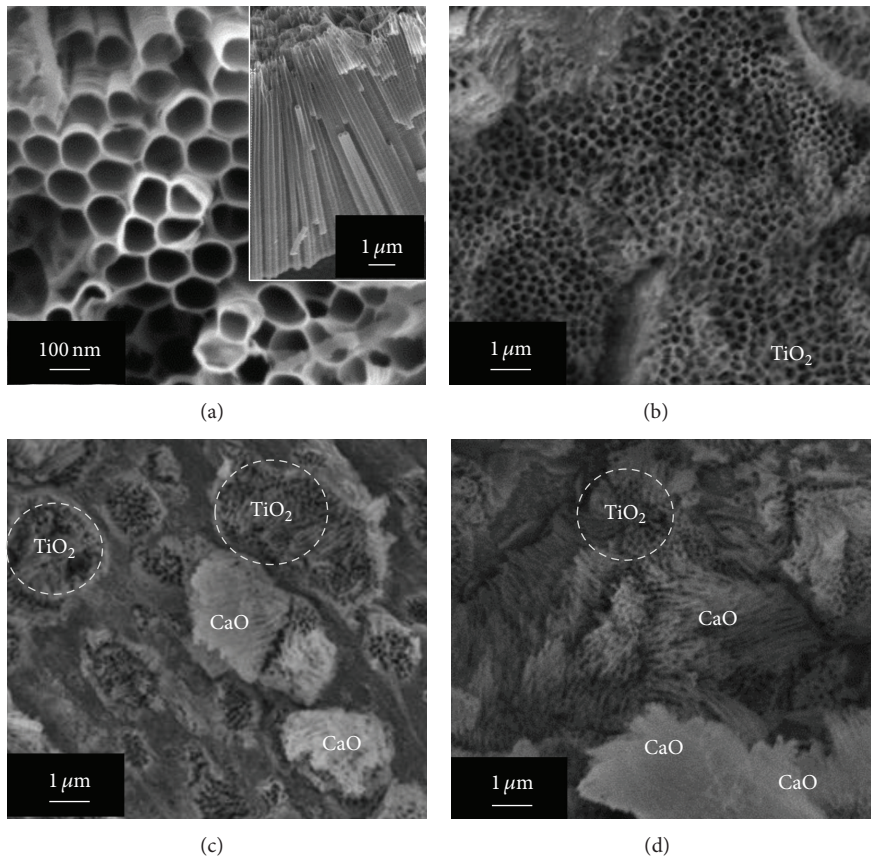

Figure 1: (a) Top view and cross-sectional view (inset) of FESEM images of pure TiO_2 nanotubes obtained; CaO-TiO_2 composite film synthesized in the electrolyte composed of different concentrations of $Ca(NO_3)_2$, (b) 0.01 M, (c) 0.05 M, and (d) 0.1 M.

morphology was observed for the sample synthesized in high concentration of 0.1 M $Ca(NO_3)_2{\cdot}4H_2O$. All nanotubes formed were collapsed and completely clogged with excessive CaO species. Then, these excessive CaO species started to accumulate on the surface of TiO_2 nanotubes. This observation indicated that the content of Ca^{2+} ions that diffused into the lattice of TiO_2 reached saturation condition and started to form independent CaO layers on the surface of nanotubes. The presence of an additional peak of Ca at 3.69 KeV was identified from EDX spectra for the CaO-TiO_2 nanotubes composite film. The intensity of the Ca peak increased with increasing concentration of $Ca(NO_3)_2{\cdot}4H_2O$ as presented in Figure 2. The atomic percentages of the Ca element within CaO-TiO_2 composite film synthesized in 0.01 M, 0.05 M, and 0.1 M $Ca(NO_3)_2{\cdot}4H_2O$ were 0.15 at%, 0.25 at%, and 0.42 at%, respectively.

In the present study, XRD analysis was used to identify the crystallographic structure and the changes in the phase structure of CaO-TiO_2 composite film. The XRD patterns of pure TiO_2 nanotubes and CaO-TiO_2 composite film as a function of the concentration of $Ca(NO_3)_2{\cdot}4H_2O$ are shown in Figure 3. The obvious diffraction peaks from the XRD pattern are attributed to the anatase phase and titanium phase. Titanium phase is originated from the substrate. The diffraction peaks at 25.32°, 38.42°, 48.02°, and 55.09° correspond to (101), (112), (200), and (211) crystal plane for the anatase phase by referring to the *JCPDS* number 21-1272 which has tetragonal crystal system. The intensity XRD peaks of anatase phase decreased after depositing with CaO dopants. These results indicated that incorporation of Ca^{2+} ions hindered the crystallization of anatase TiO_2 significantly. Interestingly, no obvious CaO phases could be detected from the XRD patterns. There could be some possible reasons, such as insensitivity of XRD instrument to identify the small content of CaO (<1 at%) or formation of amorphous CaO layer on TiO_2 nanotubes [20].

Table 1: Average elemental composition (at%) of pure TiO_2 nanotubes and CaO-TiO_2 composite film synthesized in different concentrations of $Ca(NO_3)_2{\cdot}4H_2O$.

Element $Ca(NO_3)_2{\cdot}4H_2O$ concentration	Ti (at%)	O (at%)	Ca (at%)	C (at%)
0	35.37	56.49	—	08.15
0.01	33.73	54.56	00.15	11.57
0.05	47.29	48.31	00.25	04.14
0.10	34.61	60.47	00.42	04.50

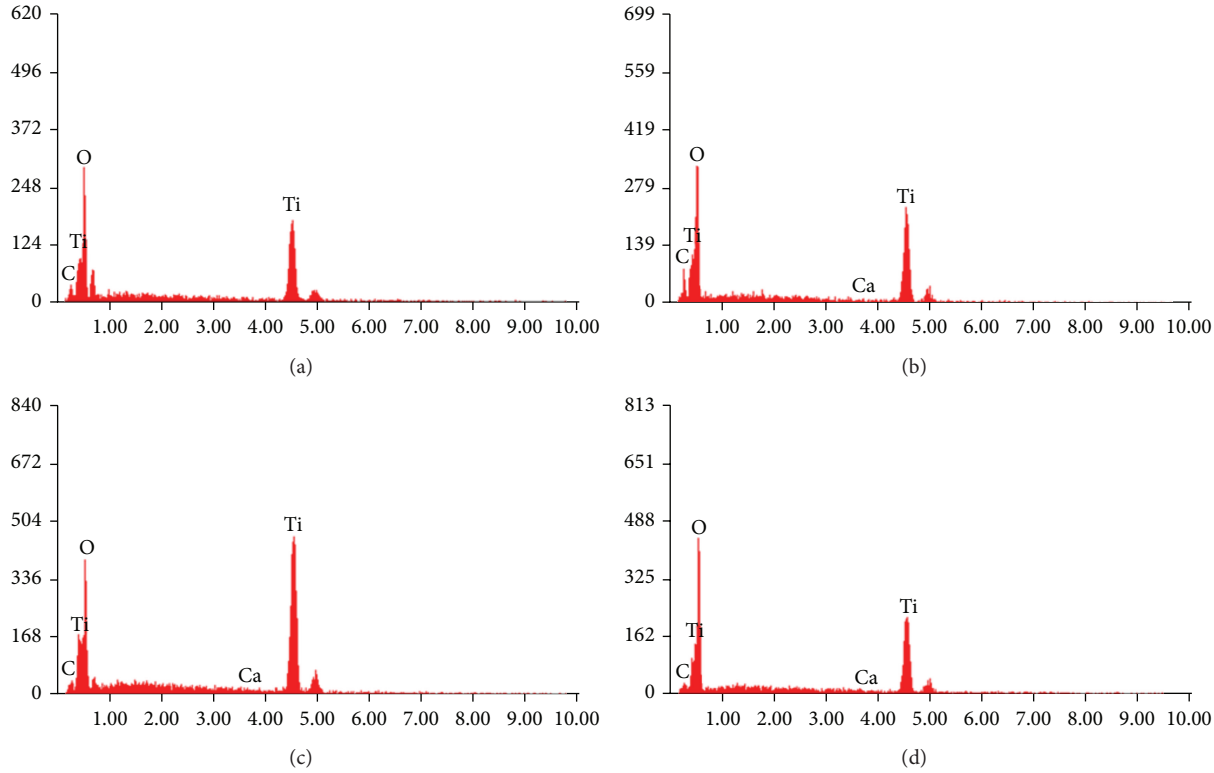

Figure 2: EDX spectra of (a) pure TiO_2 and CaO-TiO_2 composite film with different concentrations of $Ca(NO_3)_2$, (b) 0.01 M, (c) 0.05 M, and (d) 0.10 M.

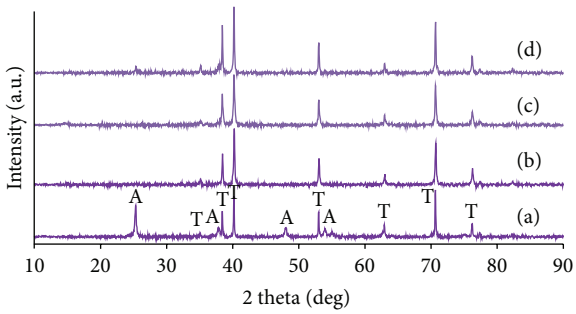

Figure 3: XRD patterns of (a) pure TiO_2 nanotubes and CaO-TiO_2 composite film produced with different concentrations of $Ca(NO_3)_2$, (b) 0.01 M, (c) 0.05 M, and (d) 0.10 M (A: anatase phase; T: titanium phase).

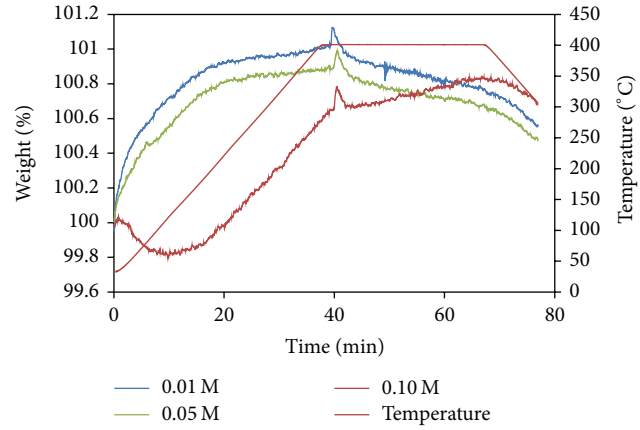

Figure 4: TGA curve of the anodized CaO-TiO_2 composite film with different concentrations of $Ca(NO_3)_2$.

Next, the resultant anodized CaO-TiO_2 composite film was used in the characterization of sorption CO_2 using TGA analysis. A N_2 gas flow at a rate of 10°C/min from room temperature (27°C up to 400°C), and then hold for 30 min in CO_2 atmosphere following by cooling down to 300°C by N_2 gas was carried out. In the present study, the carbonation stage was conducted at a lower temperature of 400°C due to the damage of nanotubular structure and phase transition at a higher temperature of 500°C [18]. The phase transition problem from anatase to rutile phase resulted in rapid growth of crystal size within the thin tube wall and eventually spoiled the nanotubular structure [21]. The TGA curves of the CaO-TiO_2 composite film with different concentrations of $Ca(NO_3)_2{\cdot}4H_2O$ are presented in Figure 4 and the CO_2 adsorption results are summarized in Table 2. It could be noticed that the CO_2 adsorption capacity is in the range from 1.89 to 2.45 mmol/g. The carbonation of CaO is through the following reaction: $CaO + CO_2 \rightarrow CaCO_3$. This reaction is reversible. A schematic illustration of basic principal CO_2 absorption using anodized CaO-TiO_2 nanotubes composite film at operating temperature of 400°C

Table 2: CO_2 adsorption capacity of the anodized CaO-TiO_2 composite film.

$Ca(NO_3)_2{\cdot}4H_2O$ concentration	CO_2 adsorption capacity (mmol/g)
0.01 M	2.45
0.05 M	1.89
0.10 M	2.36

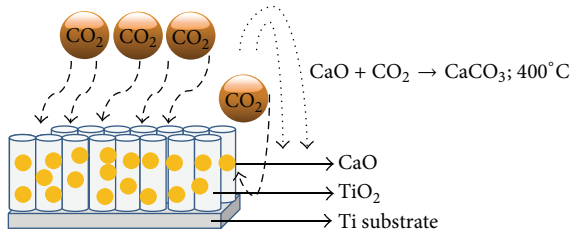

Figure 5: Schematic illustration of basic principal CO_2 absorption using anodized CaO-TiO_2 nanotubes composite film at operating temperature of 400°C.

is presented in Figure 5. In addition to that, it could be noticed that the CaO-TiO_2 nanotubes composite film (0.15 at%) synthesized in 0.01 M of $Ca(NO_3)_2{\cdot}4H_2O$ showed better CO_2 adsorption capacity of 2.45 mmol/g among the samples. This result inferred that the controlled concentration of Ca^{2+} ions within the anodization electrolyte for the formation of large active surface area of CaO-TiO_2 nanotubes is a crucial step in the improvement of CO_2 absorption. This finding might be attributed to the larger active surface area of CaO to absorb more CO_2 and simultaneous formation of $CaCO_3$. Interestingly, the sample synthesized at high concentration of 0.1 M $Ca(NO_3)_2{\cdot}4H_2O$ showed unusual patterns in TGA curve. The reason might be attributed to the fact that the nanotubular structure was collapsed and eventually formed a precipitate-like layer. Consequently, the CO_2 adsorption capacity was decreased significantly at the initial stage of carbonation process. The carbonation reaction was inhibited. This phenomenon resulted in lower weight percentage during the initial stage. However, it was found that the weight percentage was increased back at temperature of 100°C after 20 minutes of carbonation process. This result inferred that absorption of CO_2 molecules was started on anodic CaO-TiO_2 nanotubes composite film as the adsorbent weight was abruptly increased.

4. Conclusion

In summary, CaO-TiO_2 nanotubes composite film was successfully formed using rapid-anodic oxidation electrochemical anodization technique. The concentration of $Ca(NO_3)_2{\cdot}4H_2O$ played a critical role in the morphological control and content of CaO species loaded on TiO_2 nanotubes as well as CO_2 absorption ability. Well-aligned CaO-TiO_2 nanotubes composite film (0.15 at% of Ca element) enhanced the CO_2 absorption up to 2.45 mmol/g. The well distribution of CaO species throughout the TiO_2 nanotubular structure acted as an efficient CO_2 absorbent at 400°C.

Conflict of Interests

The author declares that there is no conflict of interests regarding the publication of this paper.

Acknowledgments

The author would like to thank University of Malaya for funding this research work under University of Malaya Research Grant (UMRG, RP022-2012D) and Fundamental Research Grant Scheme (FRGS, FP055-2013B).

References

[1] S. H. Schneider, "The greenhouse effect: science and policy," *Science*, vol. 243, no. 4892, pp. 771–781, 1989.

[2] Q. Wang, J. Luo, Z. Zhong, and A. Borgna, "CO_2 capture by solid adsorbents and their applications: current status and new trends," *Energy and Environmental Science*, vol. 4, no. 1, pp. 42–55, 2011.

[3] R. V. Siriwardane, M.-S. Shen, E. P. Fisher, and J. A. Poston, "Adsorption of CO_2 on molecular sieves and activated Carbon," *Energy & Fuels*, vol. 15, no. 2, pp. 279–284, 2001.

[4] Z. Yong, V. G. Mata, and A. E. Rodrigues, "Adsorption of carbon dioxide on chemically modified high surface area carbon-based adsorbents at high temperature," *Adsorption*, vol. 7, no. 1, pp. 41–50, 2001.

[5] S. Wang, S. Yan, X. Ma, and J. Gong, "Recent advances in capture of carbon dioxide using alkali-metal-based oxides," *Energy & Environmental Science*, vol. 4, no. 10, pp. 3805–3819, 2011.

[6] J.-R. Li, Y. Ma, M. C. McCarthy et al., "Carbon dioxide capture-related gas adsorption and separation in metal-organic frameworks," *Coordination Chemistry Reviews*, vol. 255, no. 15-16, pp. 1791–1823, 2011.

[7] J. Wilcox, E. Rupp, S. C. Ying et al., "Mercury adsorption and oxidation in coal combustion and gasification processes," *International Journal of Coal Geology*, vol. 90-91, pp. 4–20, 2012.

[8] C. Song, "Global challenges and strategies for control, conversion and utilization of CO_2 for sustainable development involving energy, catalysis, adsorption and chemical processing," *Catalysis Today*, vol. 115, no. 1-4, pp. 2–32, 2006.

[9] C. W. Lai and S. Sreekantan, "Study of WO_3 incorporated C-TiO_2 nanotubes for efficient visible light driven water splitting performance," *Journal of Alloys and Compounds*, vol. 547, pp. 43–50, 2013.

[10] A. R. Millward and O. M. Yaghi, "Metal-organic frameworks with exceptionally high capacity for storage of carbon dioxide at room temperature," *Journal of the American Chemical Society*, vol. 127, no. 51, pp. 17998–17999, 2005.

[11] W. Kulisch, A. Ruiz, R. Freudenstein et al., "Nanostructured materials for advanced technological applications: a brief introduction," in *Nanostructured Materials for Advanced Technological Applications*, NATO Science for Peace and Security Series B: Physics and Biophysics, pp. 3–34, 2009.

[12] G. H. A. Therese and P. V. Kamath, "Electrochemical synthesis of metal oxides and hydroxides," *Chemistry of Materials*, vol. 12, no. 5, pp. 1195–1204, 2000.

[13] Y.-K. Lai, J.-Y. Huang, H.-F. Zhang et al., "Nitrogen-doped TiO_2 nanotube array films with enhanced photocatalytic activity under various light sources," *Journal of Hazardous Materials*, vol. 184, no. 1–3, pp. 855–863, 2010.

[14] S. Sreekantan, L. C. Wei, and Z. Lockman, "Extremely fast growth rate of TiO_2 nanotube arrays in electrochemical bath containing H_2O_2," *Journal of the Electrochemical Society*, vol. 158, no. 12, pp. C397–C402, 2011.

[15] C. W. Lai and S. Sreekantan, "Dimensional control of TiO_2 nanotube arrays with H_2O_2 content for high photoelectrochemical water splitting performance," *Micro & Nano Letters*, vol. 7, no. 5, pp. 443–447, 2012.

[16] C. W. Lai, S. Sreekantan, and Z. Lockman, "Photoelectrochemical behaviour of uniform growth TiO_2 nanotubes via bubble blowing synthesised in ethylene glycol with hydrogen peroxide," *Journal of Nanoscience and Nanotechnology*, vol. 12, pp. 4057–4066, 2012.

[17] V. V. Hoang, H. Zung, and N. H. B. Trong, "Structural properties of amorphous TiO_2 nanoparticles," *European Physical Journal D*, vol. 44, no. 3, pp. 515–524, 2007.

[18] C. W. Lai and S. Sreekantan, "Higher water splitting hydrogen generation rate for single crystalline anatase phase of TiO_2 nanotube arrays," *The European Physical Journal Applied Physics*, vol. 59, no. 2, Article ID 20403, 8 pages, 2012.

[19] C. W. Lai and S. Sreekantan, "Single step formation of C-TiO_2 nanotubes: influence of applied voltage and their photocatalytic activity under Solar illumination," *International Journal of Photoenergy*, vol. 2013, Article ID 276504, 8 pages, 2013.

[20] A. K. L. Sajjad, S. Shamaila, B. Z. Tian, F. Chen, and J. L. Zhang, "One step activation of WO_x/TiO_2 nanocomposites with enhanced photocatalytic activity," *Applied Catalysis B: Environmental*, vol. 91, no. 1-2, pp. 397–405, 2009.

[21] D. Regonini, A. Jaroenworaluck, R. Stevens, and C. R. Bowen, "Effect of heat treatment on the properties and structure of TiO_2 nanotubes: phase composition and chemical composition," *Surface & Interface Analysis*, vol. 42, no. 3, pp. 139–144, 2010.